

Search for ultralight vector dark matter with a Torsion Pendulum Dual Oscillator

Ling Sun¹, Bram J. J. Slagmolen¹ and Jiayi Qin¹

¹*OzGrav-ANU, Centre for Gravitational Astrophysics, College of Science,
The Australian National University, Australian Capital Territory 2601, Australia**

(Dated: February 15, 2024)

Ultralight bosons with masses in the range from $\sim 10^{-22}$ eV to ~ 1 eV, are well-motivated, wave-like dark matter candidates. Particles on the lower-mass end are less explored in experiments due to their vanishingly small mass and weak coupling to the Standard Model. We propose to search for $U(1)_{B-L}$ gauge boson dark matter using a Torsion Pendulum Dual Oscillator (TorPeDO), a sensor originally designed to detect Newtonian gravitational field fluctuations with an enhanced differential torque sensitivity in a frequency band of $\sim 10^{-2}$ –10 Hz. We describe the experiment setup of a modified TorPeDO sensor, equipped with four 5-kg end test masses (two made from beryllium and two from aluminium). We present the estimated sensitivity to an ultralight dark matter field coupled to baryon minus lepton ($B-L$) number, in a mass range of $\sim 10^{-17}$ – 10^{-13} eV. The projected constraints on the coupling constant $g_{B-L}(\hbar c)^{-1/2}$ can reach $\sim 10^{-29}$ for a boson mass of $\sim 10^{-15}$ eV in the most sensitive frequency band.

I. INTRODUCTION

Dark matter is an essential component in astrophysics and modern cosmology [1, 2], and strong evidence for its existence has been observed from the gravitational behavior in the Universe, e.g., through gravitational lensing effects [3, 4]. Nevertheless, the nature of dark matter remains elusive. The masses of dark matter candidates span over 90 orders of magnitude [5], ranging from fuzzy dark matter (wave-like ultralight particles) with masses $\sim 10^{-22}$ eV [6, 7], weakly interacting massive particles (WIMP) with masses in the \sim GeV–TeV regime [8], to massive primordial black holes [9]. The wide spread in the mass range sets a challenge to detect the dark matter signature and requires various types of exquisitely sensitive experiments, probing different interaction mechanisms.

The lower-end mass regime is particularly difficult to explore due to the particle’s vanishing mass and is tested less with experiments. In recent years, searches for ultralight dark matter have been proposed or carried out with experiments on various scales, ranging from atomic clocks [10, 11], optomechanical cavities and laser interferometers [12–18], including kilometer-scale ground-based gravitational-wave detectors [19–22], torsion-balance accelerometers [23–26], and astrophysical approaches with black hole superradiance and pulsar timing [27–30].

Here, we focus on a well-motivated scenario: ultralight vector dark matter field coupled to the Standard Model via the baryon minus lepton ($B-L$) number. Such an ultralight vector field couples to neutrons and exerts time-oscillating, equivalence-principle-violating forces on normal matter. A recent study [26] used a single torsion balance with four beryllium (Be) and four aluminium (Al) test masses to measure the torque from a $B-L$ coupled vector dark matter field. The search put a sensitive constraint on the coupling constant $g_{B-L}(\hbar c)^{-1/2} < 1 \times 10^{-25}$

for a boson mass of $\sim 8 \times 10^{-18}$ eV/ c^2 , where \hbar is the reduced Planck constant, and c is the speed of light.

We propose to use a novel optomechanical differential torsion sensor, the Torsion Pendulum Dual Oscillator (TorPeDO) [31, 32], to search for such $B-L$ coupled vectors. TorPeDO is a mid-scale (~ 1 m) torsion pendulum detector, originally designed to continuously measure gravitational field fluctuations to mitigate Newtonian noise in terrestrial laser interferometric gravitational-wave detectors. The differential torsion sensor, with two pendulum beams, can be adapted to a dark matter detector by installing, on the two ends of each beam, equal-mass test masses made from different materials. We consider a Be test mass on one end and an Al test mass on the other end, each with a mass of 5 kg. With the \sim meter size beams and \sim kg size test masses, the sensitivity of TorPeDO can be extended to test the coupling constant at the level of $g_{B-L}(\hbar c)^{-1/2} \lesssim 10^{-28}$ in the most sensitive frequency band of 0.01–1 Hz, corresponding to a mass range of $\sim 10^{-15}$ eV/ c^2 .

The structure of the paper is as follows. We start with reviewing the vector dark matter interaction model in Sec. II. In Sec. III, we describe the TorPeDO experiment design and setup. Then, we derive the sensitivity estimates and the projected constraints on the coupling constant in Sec. IV and conclude in Sec. V.

II. VECTOR DARK MATTER FIELD

The Lagrangian of a massive vector dark matter field coupled to a number current density J^μ of baryons (B) or baryons minus leptons ($B-L$) is given by [20]

$$\mathcal{L} = -\frac{1}{4}F^{\mu\nu}F_{\mu\nu} + \frac{1}{2}m_A^2 A^\mu A_\mu - eJ^\mu A_\mu, \quad (1)$$

where m_A is the mass of the vector field, A_μ is the four-vector potential of the field, $F_{\mu\nu} = \partial_\mu A_\nu - \partial_\nu A_\mu$ is the electromagnetic field tensor, e is the electric charge, and

* ling.sun@anu.edu.au

ϵ is the gauge coupling constant normalized by the electromagnetic coupling constant.

The total energy of a dark matter particle with mass m_A is the sum of its rest energy and kinetic energy, i.e., $m_A c^2 [1 + (v_0/c)^2/2]$. The dark matter orbiting the galactic center is non-relativistic, with a typical velocity of $v_0 \approx 220$ km/s (i.e., $v_0/c \sim 10^{-3}$) [22, 33]. The oscillation frequency of the field is approximately

$$f_0 = \frac{m_A c^2}{2\pi\hbar}. \quad (2)$$

There is a small fractional deviation on the order of 10^{-7} , i.e.,

$$\frac{\Delta f}{f_0} = \frac{1}{2} \left(\frac{v_0}{c} \right)^2. \quad (3)$$

Thus, the local dark matter field can approximately be treated as a plane wave,

$$A_\mu \approx A_{\mu,0} \cos(2\pi f_0 t - \mathbf{k} \cdot \mathbf{x} + \phi), \quad (4)$$

where $A_{\mu,0}$ is the amplitude of the field, \mathbf{k} is the propagation vector, \mathbf{x} is the position vector, and ϕ is a random phase. In the non-relativistic regime, the time component A_t is negligible compared to the spatial component \mathbf{A} , and hence we ignore A_t . Here, the kinetic energy contribution is neglected, and the polarization and propagation are treated as constant vectors. Such an approximation is only valid within a duration t_c when the field is coherent, i.e.,

$$t_c \simeq \frac{1}{\Delta f} \approx \frac{1}{3 \times 10^{-7} f_0}. \quad (5)$$

We can write the dark matter electric field as

$$\begin{aligned} \mathbf{E}_A &= \partial_t \mathbf{A}(t, \mathbf{x}), \\ &= E_0 \hat{\mathbf{e}}_A \sin(2\pi f_0 t - \mathbf{k} \cdot \mathbf{x} + \phi), \end{aligned}$$

where $\mathbf{A}(t, \mathbf{x})$ is the spatial vector field at time t and position \mathbf{x} , E_0 is the amplitude of the dark matter electric field, and $\hat{\mathbf{e}}_A$ is the unit vector parallel to \mathbf{E}_A . In the non-relativistic regime, the dark matter magnetic field is negligible compared to the dark matter electric field, and E_0 can be determined by

$$E_0 = \sqrt{2\rho_{\text{DM}}}, \quad (6)$$

where $\rho_{\text{DM}} \approx 0.3$ GeV/cm³ is the local dark matter energy density [25].

In this paper, we consider a $U(1)_{B-L}$ gauge boson. The field interacts with objects carrying $B-L$ ‘‘charges’’, q_{B-L} , with a coupling constant g_{B-L} . For an object of a particular atomic species with a total mass M , the $B-L$ charge is

$$q_{B-L} = \frac{A-Z}{\mu} \frac{M}{m_n}, \quad (7)$$

where A is the atomic mass number, Z is the atomic number, μ is the atomic mass in atomic mass units, and m_n is the neutron mass. The term $(A-Z)/\mu$ stands for the neutron-to-mass ratio (i.e., charge-to-mass ratio). Analogous to the electric force, the dark matter electric force on a free-falling object with a charge q_{B-L} can be written as

$$\mathbf{F}_A = g_{B-L} q_{B-L} \mathbf{E}_A. \quad (8)$$

III. TORSION PENDULUM DUAL OSCILLATOR

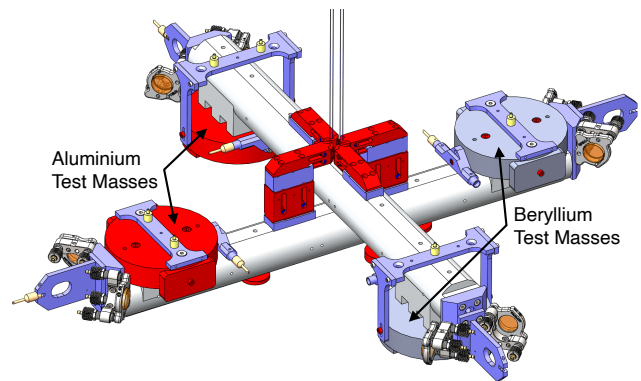


Figure 1. CAD rendering of the TorPeDO sensor. The two pendulum beams are in a cross formation. The beryllium (Be) and aluminium (Al) test masses are highlighted at the end of each beam. (The shape and size of the test masses are for demonstration purposes and do not match the actual final design.)

The TorPeDO sensor consists of two independent torsion pendulum beams, suspended in a cross formation (see Figure 1). The centers of mass of the two pendulums are designed to overlap in the three-dimensional space. Each dumbbell-like torsion pendulum consists of a 0.6-m beam with 5-kg test masses on both ends (~ 0.85 -m long in total). The length of the mechanical lever arm from the axis of rotation to the center of each test mass is 0.24 m. The total moment of inertia of each pendulum is 0.75 kg m², including the mounting equipment and hardware in addition to the test masses and the beam [34]. Each beam is suspended by two 0.6-m long, 431.8- μ m diameter, tungsten suspension wires that are attached to each pendulum at a height of ~ 0.085 m above their centers of mass (at the top of the center red blocks in Figure 1). By design, the torsion pendulums have a mechanical resonant frequency of 2.6×10^{-2} Hz. The suspension point of the two pendulums is common and provides a large suppression on mechanical common modes. A large complex mechanical suspension and isolation chain is in place to mitigate the environmental seismic motion of the suspen-

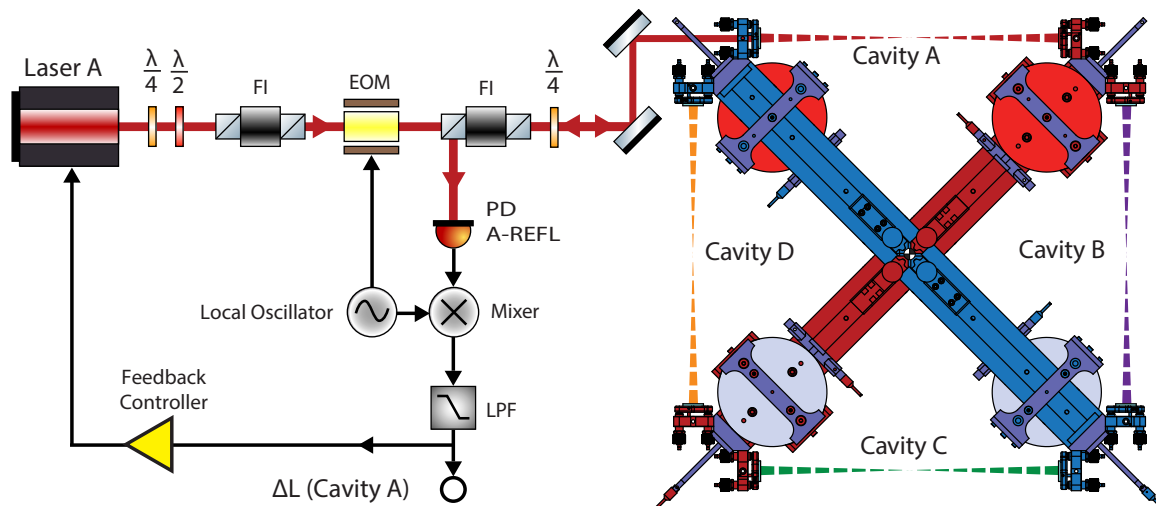


Figure 2. Optical cavities and readout of the TorPeDO sensor. Four optical cavities (A, B, C, and D) are formed between the dual torsion pendulums. In each cavity, an independent laser and the Pound-Drever-Hall (PDH) locking system are used to measure the cavity length change, ΔL . Only Cavity A system is shown in the figure for clarity. FI—Faraday Isolator, $\lambda/2$ —half wave plate, $\lambda/4$ —quarter wave plate, LPF—low pass filter, PD—photodetector, EOM—electro-optic modulator. The test masses in red and blue are made from Al and Be, respectively (see Figure 1.)

sion point down to 1.9×10^{-10} $\text{m Hz}^{-1/2}$ in displacement and 3.9×10^{-12} $\text{rad Hz}^{-1/2}$ in rotation at 0.1 Hz [32].

In this experiment, we modify the torsion beams by replacing the stainless steel test masses with two end-masses made from Be (light blue) and two end-masses made from Al (red). The vector field is weakly coupled to the Standard Model via the $B-L$ number. The force strength that a free-falling massive object experiences depends on the number of neutrons (i.e., of q_{B-L} charges) within the object, which are different per unit mass of the two atomic species, Be and Al. The difference in the charge-to-mass ratios of Be and Al is

$$\Delta_{B-L} = \frac{A_{\text{Be}} - Z_{\text{Be}}}{\mu_{\text{Be}}} - \frac{A_{\text{Al}} - Z_{\text{Al}}}{\mu_{\text{Al}}} = 0.0359, \quad (9)$$

where the subscripts denote the atomic species. The dark matter field exerts a different force on the Be test masses compared to the Al test masses, resulting in a net torque. The TorPeDO is sensitive to the vertical component of the differential torque,

$$\delta\tau_A = \mathbf{F}_A \cdot (\hat{\mathbf{z}} \times \mathbf{r}) = \frac{M}{m_n} \Delta_{B-L} g_{B-L} \mathbf{E}_A \cdot (\hat{\mathbf{z}} \times \mathbf{r}), \quad (10)$$

where \mathbf{r} is the lever arm vector.

The optical setup for measuring the differential rotation between the two pendulums is shown in Figure 2. Four optical Fabry-Pérot cavities are constructed, with their partial-reflecting mirrors placed at the ends of each beam. A differential rotation of the pendulums causes common expansion and contraction of geometrically opposite cavities. Measuring an appropriate combination of cavity length changes gives the differential rotation readout of the sensor.

Each of the four cavities has its own laser and uses the Pound-Drever-Hall (PDH) locking method to obtain the cavity length error signal [35, 36]. The PDH error signal is fed back to the laser to maintain cavity resonance. In addition, the PDH error signal is used to reconstruct the differential rotation. With each pendulum having six degrees of freedom, the sensing and control matrices are carefully measured to minimize the sensing and actuation coupling of the other modes into the differential rotation. With a cavity finesse of ~ 150 and incident laser power of 10 mW, the displacement-equivalent shot noise in the cavities is 4×10^{-18} $\text{m Hz}^{-1/2}$ at 0.1 Hz, with a 0.24-m mechanical lever arm, equivalent to a differential angular limit of 10^{-17} $\text{rad Hz}^{-1/2}$ at 0.1 Hz.

Major instrumental upgrading based on the existing setup includes the redesign of the Be/Al end test masses and beams to account for the new mass distribution, technical suspension characterisation and control, and further enhancements to electromagnetic shielding and Newtonian noise mitigation. The projected amplitude spectrum density of the differential torque at design sensitivity, denoted by $S_{\delta\tau}^{1/2}$, is presented in Figure 3 [32].

IV. SENSITIVITY TO $B-L$ COUPLED FIELD

In this section, we estimate the sensitivity to the $B-L$ coupled dark matter field using the TorPeDO setup described in Sec. III and derive the projected constraints on the coupling constant g_{B-L} .

Following Equation (10), the time-varying differential torque on average is

$$\sqrt{\langle \delta\tau_A^2 \rangle} \simeq \frac{M}{m_n} \Delta_{B-L} g_{B-L} r \sqrt{\rho_{\text{DM}}}, \quad (11)$$

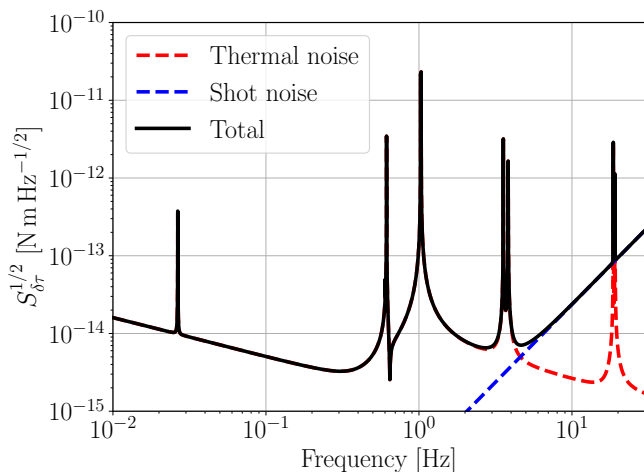


Figure 3. Projected amplitude spectrum density of the TorPeDO differential torque sensitivity. The sensitivity is limited by suspension thermal noise (red dashed curve) [32] and shot noise (blue dashed curve) at lower and higher frequencies, respectively. The five major groups of spikes, from left to right, are caused by the effective difference between the two torsion resonances, longitudinal and transverse resonances, roll resonances, pitch resonances, and vertical resonances, respectively.

where the root-mean-square amplitude of \mathbf{E}_A (i.e., $E_0/\sqrt{2} = \sqrt{\rho_{DM}}$) is used as the averaged field strength, and $r = 0.24$ m is the lever arm length. The signal-to-noise ratio (SNR) scales as

$$\text{SNR} = \frac{\sqrt{\langle \delta\tau_A^2 \rangle}}{\sqrt{S_{\delta\tau}(f)}} \sqrt{T_{\text{eff}}}, \quad (12)$$

where T_{eff} is the effective integration time. When the total observing time T_{obs} is shorter than the time over which the field can be treated as coherent, the signal power can be integrated fully coherently, and we have $T_{\text{eff}} = T_{\text{obs}}$. For long-duration observations, e.g., with $T_{\text{obs}} \sim \text{year}$, the total duration is usually divided into segments with a time length of T_{coh} , over which the signal power can be integrated coherently. The random phase only remains constant within T_{coh} , and the summation between different T_{coh} segments is incoherent. In such a semicoherent integration, we have $T_{\text{eff}} \simeq (T_{\text{obs}} T_{\text{coh}})^{1/2}$. Longer T_{coh} increases the SNR given a fixed T_{obs} . By setting SNR to unity, we have a detectable limit on the differential torque, $S_{\delta\tau}^{1/2}(f) T_{\text{eff}}^{-1/2}$.¹ Thus, we can derive the sensitivity on g_{B-L} (in units of $\sqrt{\hbar c}$) from the differential torque sensitivity limit, via

$$\frac{g_{B-L}}{\sqrt{\hbar c}} = \frac{m_n}{M \Delta_{B-L} r \sqrt{\rho_{DM} \hbar c}} \frac{\sqrt{S_{\delta\tau}(f)}}{\sqrt{T_{\text{eff}}}}. \quad (13)$$

¹ In practice, the SNR required for a confident detection is usually at the level of 5–8, which depends on the noise statistics and false alarm probability. We do not discuss the SNR threshold here for brevity.

If we assume a total observing time of $T_{\text{obs}} = 180$ day and choose T_{coh} by considering the maximum allowed coherent time at each frequency f [see Equation (5)], we have

$$T_{\text{coh}}(f) = \min\left(\frac{1}{3 \times 10^{-7} f}, 180 \text{ day}\right). \quad (14)$$

In practice, interruptions during observation due to, e.g., lock loss or maintenance, may prevent achieving the full estimated sensitivity over T_{obs} . A more conservative choice of T_{coh} is to limit the maximum coherent integration time within a day, given by

$$T'_{\text{coh}}(f) = \min\left(\frac{1}{3 \times 10^{-7} f}, 1 \text{ day}\right). \quad (15)$$

The theoretically projected search sensitivity for $T_{\text{obs}} = 180$ day is shown in Figure 4 (black band). The lower and upper bounds correspond to setting T_{coh} using Equations (14) and (15), respectively. Existing limits set by other experiments are shown for comparison. A more accurate sensitivity estimate is considered for future work, which should include as-built experimental implementations, software simulations, and rigorous analysis methods.

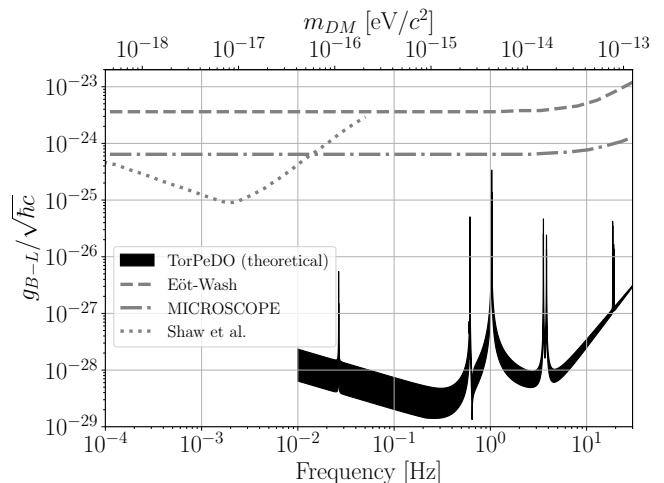


Figure 4. Theoretically projected searched sensitivity on the $B-L$ coupling constant (black band), assuming $T_{\text{obs}} = 180$ day. The lower and upper bounds correspond to setting a coherent integration time using Equations (14) and (15), respectively. The existing limits set by the Eöt-Wash experiment [37], MICROSCOPE [38], and the recent single torsion balance experiment by Shaw et al. [26], are plotted for comparison.

V. CONCLUSION

We propose the use of a differential torsion sensor, TorPeDO, to search for $B-L$ coupled ultralight vector dark matter. Such an ultralight field, if exists, would exert

equivalence-principle-violating forces on normal matter, producing accelerations that can be measured by the differential torsion sensor. The experimental setup with a \sim meter scale lever arm and \sim kg size test masses improves the sensitivity compared to existing torsion-balance experiments on a smaller scale. We demonstrate that this experiment is optimized for vector bosons in a mass range of $\sim 10^{-15}$ eV, and the theoretically projected sensitivity can enable probing the coupling constant down to $\sim 10^{-28}$ – 10^{-29} , 4–5 orders of magnitude lower than the existing constraints obtained in previously published studies.

ACKNOWLEDGMENTS

The authors thank Perry Forsyth for providing transfer function data of the TorPeDO sensor prototype. This research is supported by the Australian Research Council Centre of Excellence for Gravitational Wave Discovery (OzGrav), Project No. CE170100004.

REFERENCES

- [1] Planck Collaboration, Aghanim, N., *et al.*, *A&A* **641**, A6 (2020).
- [2] G. Bertone and D. Hooper, *Rev. Mod. Phys.* **90**, 045002 (2018).
- [3] D. Clowe, M. Bradač, A. H. Gonzalez, M. Markevitch, S. W. Randall, C. Jones, and D. Zaritsky, *The Astrophysical Journal* **648**, L109 (2006).
- [4] R. Massey, T. Kitching, and J. Richard, *Reports on Progress in Physics* **73**, 086901 (2010).
- [5] G. Bertone and T. M. P. Tait, *Nature* **562**, 51 (2018).
- [6] W. Hu, R. Barkana, and A. Gruzinov, *Phys. Rev. Lett.* **85**, 1158 (2000).
- [7] L. Hui, J. P. Ostriker, S. Tremaine, and E. Witten, *Phys. Rev. D* **95**, 043541 (2017).
- [8] M. W. Goodman and E. Witten, *Phys. Rev. D* **31**, 3059 (1985).
- [9] B. J. Carr, K. Kohri, Y. Sendouda, and J. Yokoyama, *Phys. Rev. D* **81**, 104019 (2010).
- [10] A. Arvanitaki, J. Huang, and K. Van Tilburg, *Phys. Rev. D* **91**, 015015 (2015).
- [11] C. J. Kennedy, E. Oelker, J. M. Robinson, T. Bothwell, D. Kedar, W. R. Milner, G. E. Marti, A. Derevianko, and J. Ye, *Phys. Rev. Lett.* **125**, 201302 (2020).
- [12] W. DeRocco and A. Hook, *Phys. Rev. D* **98**, 035021 (2018).
- [13] I. Obata, T. Fujita, and Y. Michimura, *Phys. Rev. Lett.* **121**, 161301 (2018).
- [14] H. Liu, B. D. Elwood, M. Evans, and J. Thaler, *Phys. Rev. D* **100**, 023548 (2019).
- [15] D. Martynov and H. Miao, *Phys. Rev. D* **101**, 095034 (2020).
- [16] A. A. Geraci, C. Bradley, D. Gao, J. Weinstein, and A. Derevianko, *Phys. Rev. Lett.* **123**, 031304 (2019).
- [17] A. Pierce, K. Riles, and Y. Zhao, *Phys. Rev. Lett.* **121**, 061102 (2018).
- [18] D. Carney, A. Hook, Z. Liu, J. M. Taylor, and Y. Zhao, *New Journal of Physics* **23**, 023041 (2021).
- [19] S. M. Vermeulen, P. Relton, H. Grote, V. Raymond, C. Afeldt, F. Bergamin, A. Bisht, M. Brinkmann, K. Danzmann, S. Doravari, V. Kringel, J. Lough, H. Lück, M. Mehmet, N. Mukund, S. Nadji, E. Schreiber, B. Sorazu, K. A. Strain, H. Vahlbruch, M. Weinert, B. Willke, and H. Wittel, *Nature* **600**, 424 (2021).
- [20] Y. Michimura, T. Fujita, S. Morisaki, H. Nakatsuka, and I. Obata, *Phys. Rev. D* **102**, 102001 (2020).
- [21] H.-K. Guo, K. Riles, F.-W. Yang, and Y. Zhao, *Communications Physics* **2**, 155 (2019).
- [22] R. Abbott *et al.* (LIGO Scientific Collaboration, Virgo Collaboration, and KAGRA Collaboration), *Phys. Rev. D* **105**, 063030 (2022).
- [23] S. Schlamminger, K.-Y. Choi, T. A. Wagner, J. H. Gundlach, and E. G. Adelberger, *Phys. Rev. Lett.* **100**, 041101 (2008).
- [24] T. A. Wagner, S. Schlamminger, J. H. Gundlach, and E. G. Adelberger, *Classical and Quantum Gravity* **29**, 184002 (2012).
- [25] P. W. Graham, D. E. Kaplan, J. Mardon, S. Rajendran, and W. A. Terrano, *Phys. Rev. D* **93**, 075029 (2016).
- [26] E. A. Shaw, M. P. Ross, C. A. Hagedorn, E. G. Adelberger, and J. H. Gundlach, *Phys. Rev. D* **105**, 042007 (2022).
- [27] L. Sun, R. Brito, and M. Isi, *Phys. Rev. D* **101**, 063020 (2020).
- [28] R. Abbott *et al.* (The LIGO Scientific Collaboration, the Virgo Collaboration, and the KAGRA Collaboration), *Phys. Rev. D* **105**, 102001 (2022).
- [29] A. Khmelnitsky and V. Rubakov, *Journal of Cosmology and Astroparticle Physics* **2014**, 019 (2014).
- [30] N. K. Porayko and K. A. Postnov, *Phys. Rev. D* **90**, 062008 (2014).
- [31] D. J. McManus, P. W. F. Forsyth, M. J. Yap, R. L. Ward, D. A. Shaddock, D. E. McClelland, and B. J. J. Slagmolen, *Classical and Quantum Gravity* **34**, 135002 (2017).
- [32] S. S. Y. Chua, N. A. Holland, P. W. F. Forsyth, A. Kurlur Ramamohan, Y. Zhang, J. Wright, D. A. Shaddock, D. E. McClelland, and B. J. J. Slagmolen, *Applied Physics Letters* **122**, 201102 (2023).
- [33] M. C. Smith, G. R. Ruchti, A. Helmi, R. F. G. Wyse, J. P. Fulbright, K. C. Freeman, J. F. Navarro, G. M. Seabroke, M. Steinmetz, M. Williams, O. Bienaymé, J. Binney, J. Bland-Hawthorn, W. Dehnen, B. K. Gibson, G. Gilmore, E. K. Grebel, U. Munari, Q. A. Parker, R.-D. Scholz, A. Siebert, F. G. Watson, and T. Zwitter, *Monthly Notices of the Royal Astronomical Society* **379**, 755 (2007).
- [34] P. W. F. Forsyth, *Simulation and isolation design for the TorPeDO gravitational sensor*, Ph.D. thesis, The Australian National University (2022).
- [35] R. W. P. Drever, J. L. Hall, F. V. Kowalski, J. Hough, G. M. Ford, A. J. Munley, and H. Ward, *Applied Physics B* **31**, 97 (1983).
- [36] E. D. Black, *American Journal of Physics* **69**, 79 (2001).
- [37] S. Schlamminger, K.-Y. Choi, T. A. Wagner, J. H. Gundlach, and E. G. Adelberger, *Phys. Rev. Lett.* **100**, 041101 (2008).
- [38] J. Bergé, P. Brax, G. Métris, M. Pernot-Borràs, P. Touboul, and J.-P. Uzan, *Phys. Rev. Lett.* **120**, 141101 (2018).